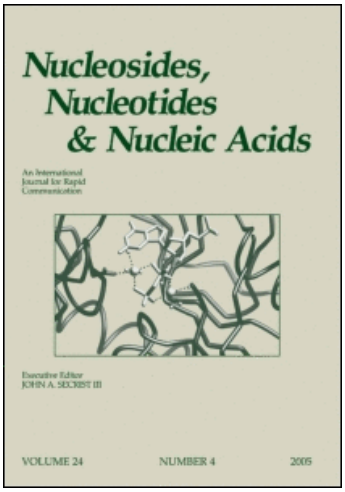

Nucleosides, Nucleotides and Nucleic Acids
Publication details, including instructions for authors and subscription information:
http://www.informaworld.com/smpp/title~content=t713597286

Conformational Properties of Nucleotide-Based Template-Competitive HIV-1 Reverse Transcriptase Inhibitors: Analysis of Enzyme Binding Modes

Weiying Lin[a]; Ke Li[a]; Bob M. Moore II[ab]; Michael B. Doughty[ac]
[a] Department of Chemistry and Physics, Southeastern Louisiana University, Hammond, Louisiana, USA [b] Department of Pharmaceutical Sciences, University of Tennessee Health Science Center, Memphis, TN, USA [c] Department of Chemistry and Physics, Southeastern Louisiana University, Hammond, LA, USA

Online publication date: 05 December 2003

To cite this Article Lin, Weiying , Li, Ke , Moore II, Bob M. and Doughty, Michael B.(2003) 'Conformational Properties of Nucleotide-Based Template-Competitive HIV-1 Reverse Transcriptase Inhibitors: Analysis of Enzyme Binding Modes', Nucleosides, Nucleotides and Nucleic Acids, 22: 3, 283 — 297
To link to this Article: DOI: 10.1081/NCN-120021428
URL: http://dx.doi.org/10.1081/NCN-120021428

NUCLEOSIDES, NUCLEOTIDES & NUCLEIC ACIDS
Vol. 22, No. 3, pp. 283–297, 2003

Conformational Properties of Nucleotide-Based Template-Competitive HIV-1 Reverse Transcriptase Inhibitors: Analysis of Enzyme Binding Modes[#]

Weiying Lin, Ke Li, Bob M. Moore II,[‡] and Michael B. Doughty[*]

Department of Chemistry and Physics, Southeastern Louisiana University, Hammond, Louisiana, USA

ABSTRACT

Nucleotides 2-(4-azidophenacyl)thio-1,N^6-etheno-2′-deoxyadenosine 5′-triphosphate **1** and its tetrafluoro analog **2** inhibit HIV-1 reverse transcriptase (RT) competitively relative to template. These template-competitive RT inhibitors (TCRTIs) were analyzed for conformational properties by molecular modeling and NMR analysis. Both inhibitors prefer sugar conformations of $C_{2'}$-endo/$C_{3'}$-exo with a high-anti glycosidic bond rotation and +sc/ap phosphate conformation (γ). The major effect of the etheno group is to favor an extended, fully staggered anti conformation in the N1-C2-S-CH_2 ψ_1 side chain rotation,

[#]Taken in part from the dissertations of Dr. Weiying Lin, The University of Kansas, 2000; Dr. Ke Li, The University of Kansas, 1996; and Dr. Bob M. Moore II, The University of Kansas, 1995.

[‡]Current affiliation: Department of Pharmaceutical Sciences, University of Tennessee Health Science Center, Memphis, TN 38163, USA.

*Correspondence: Michael B. Doughty, Department of Chemistry and Physics, Southeastern Louisiana University, SLU Box 10878, Hammond, LA 70402, USA; Fax: (985) 549-5126; E-mail: mdoughty@selu.edu.

DOI: 10.1081/NCN-120021428
1525-7770 (Print); 1532-2335 (Online)

and NMR analysis detects a long range sugar $H_{4'}$ to side chain phenyl *meta*-H NOE, a result consistent with this compact structure as an important contributor to the solution structure. The binding model generated places the phenyl side chain in a lipophilic pocket in the template grip region of the RT polymerase domain with the Mg-triphosphate complexed to active site carboxylates. The structures of the TCRTIs are compared with that of the template-competitive DNA polymerase inhibitor 2-(4-azidophenacyl)thio-2′-deoxyadenosine 5′-triphosphate **3**, and a theoretical model for selectivity is proposed.

Key Words: Nucleotide conformation; Reverse transcriptase; DNA polymerase; Template-competitive inhibitors; Combined-substrate inhibitors.

INTRODUCTION

Nucleotide conformations are often an important determinant of substrate and inhibitor binding to nucleotide and nucleic acid processing enzymes. For example, conformational properties of nucleoside reverse transcriptase (RT) inhibitors, in particular AZT, taken from x-ray crystallography,[1] NMR spectroscopy,[2] and various potential energy calculations[1] provided important structure-activity information. We are similarly interested in the conformations of our recently reported nucleotide inhibitors of both HIV-1 reverse transcriptase (RT) and *E. coli* DNA polymerase I Klenow fragment (Pol I)[3,4] These nucleotides were designed as combined-substrate inhibitors with binding interactions at both the dNTP and template binding sites of the respective enzymes.

The template-competitive RT inhibitors (TCRTIs), exemplified by 2-(4-azidophenacyl)thio-1, N^6-etheno-2′-deoxyadenosine 5′-triphosphate **1** and the tetrafluoro analog **2**, inhibit HIV-1 RT competitively relative to template-primer (and thus the name), and photolabel and photoinactivate the free enzyme.[3] The phenylazide of both **1** and **2** label RT in the template-grip, a region of RT found important for binding and positioning of the template during reverse transcription.[5] The template-competitive Pol I inhibitor (TCPI) 2-(4-azidophenacyl)thio-2′-deoxyadenosine 5′-triphosphate **3** was characterized kinetically as a reversible inhibitor and as a photoprobe. This inhibitor binds to the free enzyme form of Pol I with a low to sub-micromolar affinity, but is not a substrate since it does not bind to the enzyme-template/primer binary complex.[4] Additionally, the azidophenacyl group photolabels a lipophilic site at the junctures of helices M, N, and O in the template binding domain.[6]

A most interesting difference between the RT inhibitors **1** and **2** and the Pol I inhibitor **3** is that they show considerable selectivity. Thus TCRTIs **1** and **2** are >800-fold more active than **3** as an RT inhibitor, and **3** is 100 times more active as a DNA pol inhibitor reltaive to **1**. This >80,000 fold switch in selectivity is difficult to explain based on a simple model in which the etheno group increases the lipophilicity of the purine ring. In order to understand the potential impact of the 1,N^6-etheno group on this selectivity, we investigated the structural properties of the RT inhibitors **1** and **2** relative to the structural properties of **3** reported earlier.[6] In the present communication we demonstrate that the discernable structural

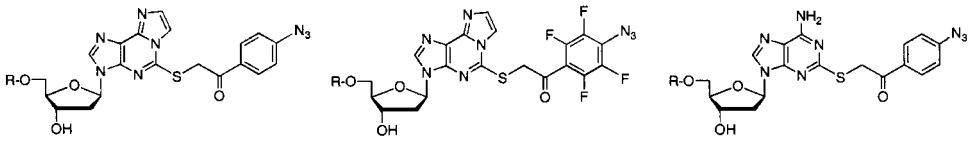

1 R = $P_3O_9H_4$
1m R = PO_3H_2

2 R = $P_3O_9H_4$
2m R = PO_3H_2

3 R = $P_3O_9H_4$
3m R = PO_3H_2

difference between the TCRTIs **1** and **2** and the DNA pol inhibitor **3** is an effect of the etheno group on the 2-side chain conformation, and we also provide an enzyme structural model that rationalizes the selectivity observed.

EXPERIMENTAL

1. Computational Methods

Sybyl 6.0 (Tripos Associates, Inc., St. Louis, MO) computations were run on an IBM RS/600 Workstation Model 560 or a Silicon Graphics O2 workstation. Nucleotide inhibitors were modeled using Sybyl by modification of the structure of dAMP taken from BIOPOLYMER. Semi-empirical calculations were performed using the MOPAC package and MNDO method in Sybyl 6.0 to optimize the charge and geometry of nucleotide analogues. Potential energy calculations of adenine analogues were performed using the Tripos force field, and those of nucleotide analogues were performed using the Kollman all atom force field[7,8] with addition of the $C_{4'}$-$O_{4'}$-$C_{1'}$-N^* anomeric torsional parameters for cyclic compounds to correct for the anomeric effect.[9] A dielectric constant of 1 was used in these calculations. Systematic sampling of torsional space was accomplished using the GRID SEARCH option in Sybyl 6.0, which allows complete optimization of the molecule at each increment except for the torsional angle being driven. The criterion for termination of minimization was an energy change less than 0.0001 kcal/mol. The conformations generated by grid search were analyzed using the MOLECULAR SPREADSHEET function in Sybyl 6.0, which allows the measurement and calculation of various parameters, such as torsional angles, interproton distances, and the pseudorotational phase angle P. Docking studies were performed using Midas[10] running on a Silicon Graphics Indigo workstation. Protein structures (1HVT superseded by 2HVT for RT; 1DPI for DNA polymerase I Klenow fragment) were obtained from Brookhaven protein database.[11] The triphosphate crystal structure was taken from ADENTP from the CSD (CCDC, Cambridge. CB2 1EZ. UK).

2. Nuclear Magnetic Resonance Spectroscopy

Nucleotide samples were dissolved in D_2O at final concentrations of 1–5 mM. ^1H NMR spectra were recorded at 25°C on a Bruker AM 500 NMR spectrometer. Vicinal proton-proton coupling constants of the furanose ring were measured by sequential decoupling of furanose protons at 288, 298, and 306 K, respectively.

PSEUROT BASIC calculations were performed using the generalized Karplus equation (1):

$$^3J_{HH} = P_1 \cos^2 \phi_j + P_2 \cos \phi_j + P_3 + \Sigma\Delta\chi_i\{P_4 + P_5 \cos^2(\xi_i\phi_j + P_6|\chi_i|)\} \quad (1)$$

where $^3J_{HH}$ is the vicinal proton-proton coupling constants, P_1 to P_6 are constants determined by a least-squares procedure using 315 model compounds, ϕ_j is the dihedral angle, ξ_i is a constant that has a value of +1 or −1 depending on the orientationof the substituent relative to its geminal proton, and $\Delta\chi_i$ is the difference of the Huggins electronegativity between the substituent i and hydrogen.[12] In addition, the primary (α) $\Delta\chi_i$ values are influenced by β substituents as expressed by equation (2):

$$\Delta\chi^{\text{group}} = \Delta\chi^{\alpha\text{ substituent}} - P_7\Sigma\Delta\chi_j^{\beta\text{ substituent}}$$

where P_7 is a constant and the summation is over all the substituents j bound to substituent i.[13]

Phase sensitive two dimensional ROESY spectra were acquired with time proportional phase incrementation and a mixing time of 500 ms. Data were accumulated with 64 scans/block containing 4 dummy scans for 256 blocks, a 4000 Hz sweep width, and a 2 s relaxation between scans, collecting 2 K data points. Data was then transferred to a Silicon Graphics Indigo work station and multiplied by a shifted sine-bell weighting function in both dimensions. The spectra were Fourier transformed using Felix NMR data processing software (Biosym, San Diego, CA).

RESULTS AND DISCUSSION

1. Molecular Mechanics Conformational Analysis of Nucleotides 1 and 2

Side Chain Conformational Analysis

The four rotatable bonds in the phenacyl side chains of **1**, **2**, and **3** are named Ψ_1, Ψ_2, Ψ_3, and Ψ_4 as illustrated in Fig. 1. Systematic energy minimization by rotation of the torsional angles in the corresponding base of TCRTIs **1** and **2** were carried out using molecular mechanics calculations not including the azido group as previous results have shown that it has little effect on the structure and dipole moment.[4] The charges and geometry of 2-phenacylthio-1,N^6-etheno-adenine and 2-(2,3,5,6-tetrafluoro)phenacylthio-1,N^6-etheno-adenine were determined by MOPAC calculations using the MNDO method. The energy calculations were then performed for each rotatable bond using a grid search in which the torsional angle was driven from −180° to 180° by an increment of 5° with the other three torsional angles starting from a fully extended, *anti*, conformation.

The energy profiles for Ψ_1 of **1** and **2** generated from these calculations, as well as the Ψ_1 plot for TCPI **3**, are shown in Fig. 2. As predicted, torsional angle Ψ_1 had an energy *maximum* at 0° where the etheno group is eclipsed with the methylene group of the side chain. However, an energy *minimum* was observed at 180°, in which

Marcel Dekker, Inc.
270 Madison Avenue, New York, New York 10016

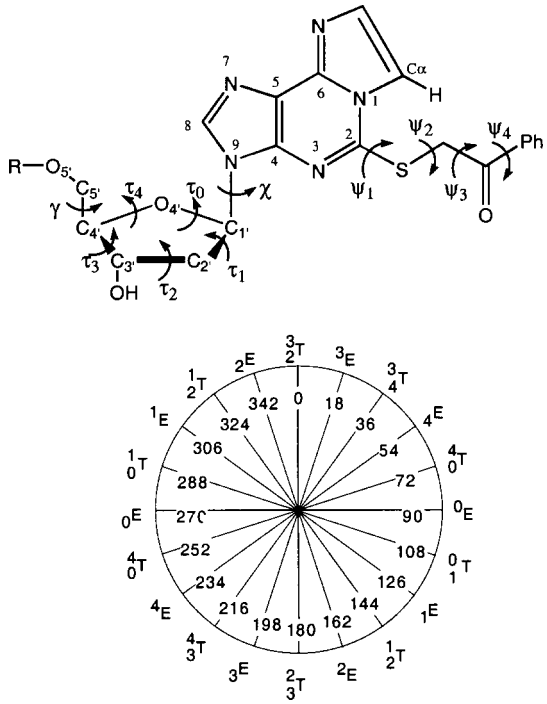

Figure 1. Conformational Properties of Nucleotides. Top: Definition of conformational rotations in a representative nucleotide; $\gamma = C_{3'}\text{-}C_{4'}\text{-}C_{5'}\text{-}O_{5'}$; $\chi = O_{4'}\text{-}C_{1'}\text{-}N9\text{-}C4$, $\psi_1 = N1\text{-}C2\text{-}S\text{-}CH_2$. Bottom: Pseudorotational cycle, where the conformations are listed outside the circle and the corresponding pseudorotation phase angles (P) are listed inside the circle; ${}^{m}E$ = endo, or up, conformation, ${}_{n}E$ = exo, or down, conformation, and ${}^{m}_{n}T$ = twist conformation where n and m define the atom(s) involved.

the methylene group is anti to the etheno ring and eclipsed with the N3 lone pair. The preference for the 180° conformer was somewhat unexpected since the side chain rotation in the adenine analog **3** showed a strong preference for the −90 and +90° conformers (by about 8 kcal/mol) where the methylene group of the side chain

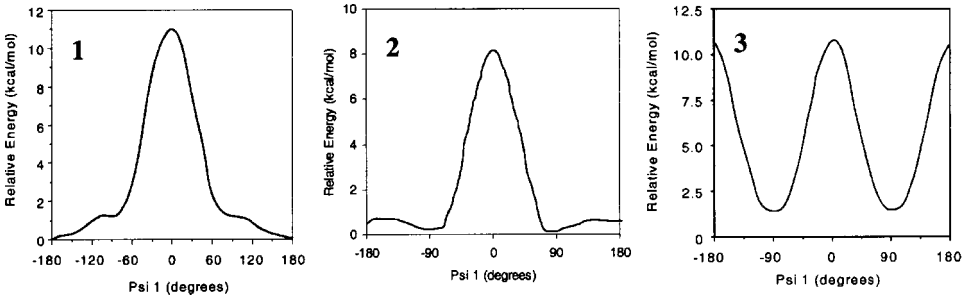

Figure 2. Grid search plots for rotation about Psi 1 for TCRTIs **1** (left) and **2** (center), and for the DNA polymerase inhibitor **3** (right).

Marcel Dekker, Inc.
270 Madison Avenue, New York, New York 10016

projects out from the plane of the adenine ring (Fig. 2, right graph). The slight preference (about 1.5 kcal/mol) for the 180° *anti* conformer preference in **1** is likely due to the lone pairs on sulfur, since in the 180° rotation the lone pairs are staggered and gauche to the etheno CH, whereas in the 90° conformation one lone pair is near eclipsed to the etheno. This preference for the 180° conformation of the side chain is the major discernable structural difference between **1** vs **3** as RT vs DNA pol inhibitors, respectively. The side chain preference of TCRTI **2** resembles that of the TCRTI **1** with the exception that the +90 and −90 conformers show a < 0.5 kcal/mol preference over the +180° conformer, but the 0° conformer is strongly disfavored.

Torsional angles Ψ_2 and Ψ_3 in both RT inhibitors **1** and **2** each had similar conformational preferences with energy minima near 60, −60, and 180°, corresponding to three staggered conformations (Fig. 3). The energy maxima at −120, 0, and 120 for Ψ_2 and Ψ_3 correspond to the eclipsed conformations with the highest-energy conformation at 0° reflecting the eclipsing of the alkyl (or aryl) groups. For Ψ_4, energy minima were observed near 0 and 180°, where maximum overlap between the π-electrons of the carbonyl group and those of the phenyl ring occur. Energy maxima for Ψ_4 were near 90 and −90°, where the π-electrons of the carbonyl group are perpendicular to that of the phenyl ring. Overall, these potential energy calculations give a fully extended side chain projecting at 180° from the etheno group as the global energy minimum conformation. However, local energy minimum conformations that have one torsional angle at –65 or 65° (Ψ_2 or Ψ_3) and the remaining three torsional angles at 180° had only slightly higher energy (about 0.2 kcal/mol).

Furanose Ring Puckering

The conformational states of the furanose ring of nucleotide inhibitors **1** and **2** were examined by computation of relative energy as a function of pseudorotation phase angle P. Phase anlge P is defined based on the interrelationship between the torsional angles of a five-membered ring using Eq. (3):[14]

$$\tan P = \frac{(\tau_4 + \tau_1) - (\tau_3 + \tau_0)}{2^{*}\tau_2\ ^{*}(\sin 36^\circ + \sin 72^\circ)} \tag{3}$$

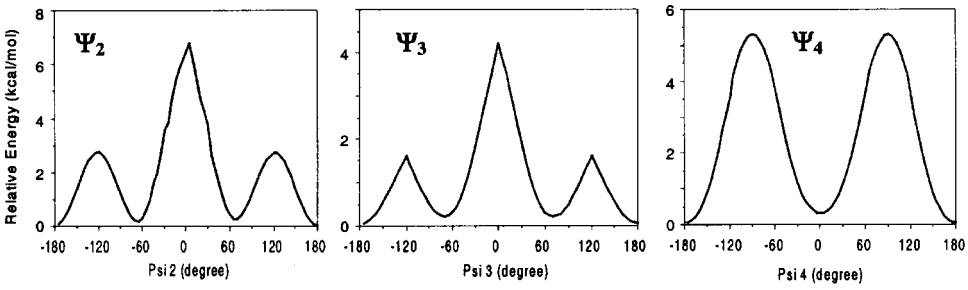

Figure 3. Conformation energy plots for side chain torsional bonds ψ_2 (left), ψ_3 (middle), and ψ_4 (right) for TCRTI **1**.

Marcel Dekker, Inc.
270 Madison Avenue, New York, New York 10016

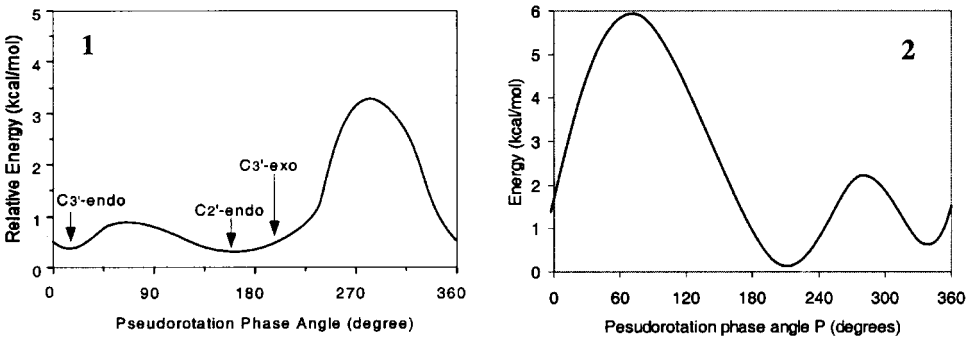

Figure 4. Pseudorotational phase angle plots for **1** (left) and **2** (right). The puckering modes are shown on the left graph. The pseudorotational angle is defined in Fig. 1 and calculated from Eq. (3).

where τ_0 to τ_4 are endocyclic torsional angles of the furanose ring with the subscript representing the first atom of the rotatable bond (see Fig. 1). Molecular mechanics calculations were performed using the Kollman all-atom force field[7,8] which has been successful in the computation of nucleic acid energetics and reproduced nucleoside pseudorotational potentials with addition of parameters for the OCN anomeric effect.[9] Grid searches were performed in which an endocyclic torsional angle of the furanose ring was driven from $-40°$ to $40°$ by an increment of $3°$. Similar grid searches were repeated for each endocyclic torsional angle of the furanose ring, and the confromations generated from these searches were tabulated. Pseudorotational phase angle P values for each conformation were then calculated by Eq. (3) to give the energy profile for the entire pseudorotational pathway as shown in Fig. 4 for **1** (left) and **2** (right).

For TCRTI **1**, the conformational analysis was performed with torsional angles χ and γ starting at *anti* and +sc, respectively, and the 2-position side chain starting in the fully extended conformation. Under these starting conditions two energy minima at $C_{2'}$-endo ($P = 160°$) and $C_{3'}$-endo ($P = 10°$) were observed with the $C_{2'}$-endo as the global energy minimum, although the energy difference between $C_{2'}$-endo and $C_{3'}$-endo was only 0.2 kcal/mol, and the minimum at $C_{2'}$-endo was broad and includes $C_{3'}$-exo. A western potential energy barrier ($P = 270°$) of about 3 kcal/mole and an eastern energy barrier ($P = 90°$) of about 0.5 kcal/mol were observed.

The global energy minimum for **2** was observed at $P = 209°$, corresponding to $C_{3'}$ exo sugar puckering, which is also the sugar conformation of B DNA (Fig. 4, bottom). Interestingly, the favorable sugar pucker of **2** is very close to the reported sugar conformation ($P = 215°$) of AZT.[15] Another energy minimum about 1 kcal/mole higher than the global minimum occurs at $P = 324°$, indicating $C_{2'}$ exo or twist sugar conformation. The eastern ($P = 75°$) and western ($P = 280°$) potential energy barriers are about 8.1 and 2.5 kcal/mol, respectively.

These calculations for both **1** and **2** are consistent with reported furanose conformational preferences,[16] as well as the sugar conformation found in B-DNA,[17]

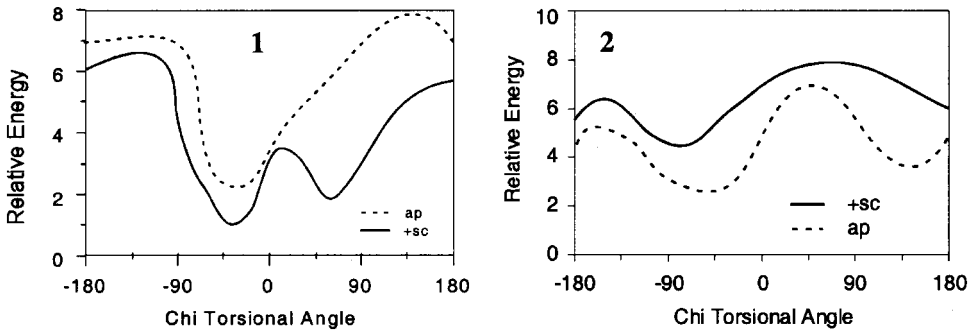

Figure 5. Chi torsional angle ($O_{4'}$-$C_{1'}$-N9-C4 as indicated in Fig. 1) energy plots for **1** (left) and **2** (right).

indicating that the structural modifications on the ethenoadenine ring in **1** and **2** do not exert a major effect on the conformational states of the furanose ring. In addition, TCPI **3** gave a predominate $C_{3'}$-exo conformation with $P = 192°$, and NMR analysis of the solution structure of **3** was consistent with this model.[6]

Glycosidic Torsional Angle Preferences

Energy profiles of TCRTIs **1** and **2** relative to χ (defined as $O_{4'}$-$C_{1'}$-N9-C4 in Fig. 1) were examined using grid searches in which χ was driven from $-180°$ to $180°$ by an increment of $5°$. The conformation of the furanose ring was first set at $C_{3'}$-exo and energy minimum conformations of the side chain with the torsional angle γ at either +sc or ap but not $-$sc since the later is rarely observed.[18] Figure 5 shows the energy profiles for **1** (left) and **2** as a function of both the +sc and ap starting conformations at γ. For all the starting side chain conformations, the +sc conformation was favored over the ap conformation and the energy-minimum fell in the range of $\chi = -35$ to $-60°$, corresponding to the high *anti* conformation, for **1**. However for **2** there was a preference for the high anti conformation in the ap rather than the +sc conformation. The preference for high *anti* conformer in **2** is consistent with the preferences for **1** and **3**,[6] but the preference for the ap conformation is not readily apparent. The NMR studies (see later) however are consistent with the calculations of a preferred ap conformation in **2**. In either case, because the discrepancy is between the two TCRTIs, this difference cannot be the origin of the selectivity differences observed.

Previous studies have demonstrated that orientation of the base about the glycosyl bond (χ) in a nucleoside is affected by sugar puckering. Purine nucleosides with $C_{2'}$-endo pucker adopt both *syn* and *anti* forms in nearly equal distribution, whereas $C_{3'}$-endo puckering favors the *anti* conformation.[18] The high anti conformation here for the $C_{3'}$-exo starting position is strengthened by the 2-side chain which introduces a steric effect in the syn conformers. In this regard, some conformations with χ in the range of 0 to $45°$ were not possible due to steric interactions between the side chain and sugar.

Marcel Dekker, Inc.
270 Madison Avenue, New York, New York 10016

2. Solution Conformations of 1 and 2 by NMR Analysis

The generalized Karplus equation, which relates the vicinal proton-proton coupling constants of the furanose ring to the dihedral angles, has been used to examine the conformational states of the furanose rings of nucleosides and nucleotides. A number of methods have been developed to calculate dihedral angles and endocyclic torsion angles from proton coupling constants. The ''Dihedral Angle Estimation by the Ratio Method'' (DAERM) is based on the assumption that the ratio of Karplus constants is constant although the magnitudes vary. Two shortcomings associated with this method are: 1) there is only partial compensation for electronegative substituents, and 2) DAERM calculations give only an average of contributing conformations. The program PSEUROT (in Fortran) assumes an equilibrium between two puckering modes and calculates the phase angle P, the puckering amplitude, and the molar fraction of the two conformers.[13,14] Our lab developed PSEUROT BASIC which runs in a DOS environment and performs a global search of all possible starting conformations. The furanose ring puckering states of TCRTIs **1** and **2** were investigated by this method as an independent means of arriving at energy minimum conformations.

The vicinal proton-proton coupling constants measured by ^{1}H-NMR are given in Tables 1 and 2 for **1** and **2**, respectively. The results of PSEUROT calculations (Table 3) gave $C_{3'}$-exo ($P = 192°$) as the major conformer (75.4%) and $C_{3'}$-endo ($P = 0.8°$) as the minor conformer (24.6%) with puckering amplitudes τ_m of 18 and 40, respectively, for **1**. The $C_{3'}$-exo conformation predicted from the NMR data is

Table 1. Sugar vicinal coupling constants for **1**.

	Temperature		
Coupling	288 K	298 K	306 K
$H_{1'}$-$H_{2'}$	7.70	7.75	7.50
$H_{1'}$-$H_{2''}$	6.30	6.10	6.70
$H_{2'}$-$H_{3'}$	5.90	5.50	6.10
$H_{2''}$-$H_{3'}$	3.00	2.44	3.05
$H_{3'}$-$H_{4'}$	2.20	1.80	2.40

Table 2. Sugar vicinal coupling constants for **2**.

	Temperature		
Coupling	288 K	298 K	306 K
$H_{1'}$-$H_{2'}$	5.30	4.45	4.60
$H_{1'}$-$H_{2''}$	7.00	7.55	6.44
$H_{2'}$-$H_{3'}$	2.40	0.75	2.60
$H_{2''}$-$H_{3'}$	5.10	4.55	5.70
$H_{3'}$-$H_{4'}$	0.75	0.75	0.75

Marcel Dekker, Inc.
270 Madison Avenue, New York, New York 10016

Table 3. Results of Pseurot calculations from NMR coupling data for **1**, **2**, and **3**[a].

Inhibitor	South conformer		North conformer		% South	Predominate conformer
	P	Phase	P	Phase		
1	192°	18	0.80°	40	75%	$C_{3'}$-exo
2	205°	38	25°	27	94%	$C_{3'}$-exo
3	189°	36	342°	38	80%	$C_{3'}$-exo

[a]See Ref.[6].

consistent with the molecular mechanics calculation which predicts a broad global minimum as the south conformation which includes both $C_{2'}$-endo and $C_{3'}$-exo conformations for **1**. For **2** the calculations indicated a $C_{3'}$- exo conformer at P = 205° with ring pucker of 38 as the prodominate conformation and a minor conformer at P = 25° with a ring pucker of 27. The $C_{3'}$ exo sugar pucker as the major conformer derived from NMR studies is also in good agreement with the prediction of molecular mechanics calculations that $C_{3'}$ exo is the global energy minimum conformer. The TCPI **3** also gives a $C_{3'}$ exo conformation as the major conformer in solution, such that we conclude that the etheno substituent has little effect on the solution structure of the TCRTI sugar conformations.

The conformations of TCRTIs **1** and **2** were further analyzed by ROESY experiments which provide information on the relative spatial relationship between the protons. The NOE intensities of the ROESY plot were assigned as strong, medium, and weak, which are defined as distances of 2-3, 2-4 and 2-5 Å, respectively, relative to the intensity of the $C_{2'}H$-$C_{2''}H$ (~1.8 Å) and ArH-ArH' (~2.5 Å) enhancements (Table 4).[19] The medium sugar-base proton $H_{1'}$-H8 and $H_{2'}$-H8 NOEs, and the weak sugar-base proton $H_{3'}$-H8 NOE are all consistent with a high anti conformer. The absence of a sugar-base proton $H_{5'}$-H8 NOE is consistent with a +sc

Table 4. NOEs observed for **1**, **2**, and **3** in D_2O.

Inhibitor	Component(s)	Strong NOE	Medium NOE	Weak NOE
1	intra-sugar	1′-2″[a], 2′[b]-2″,2′-3′,3′-5′	1′-4′	–[c]
	sugar-base	–	1′-8, 2′-8	3′-8
	intra-side chain	*ortho-meta*	–	–
	sugar-side chain	–	1′-*ortho*	4′-*meta*
2	intra-sugar	2′-2″, 3′-4′, 3′-5′	1′-2″, 1′-3′	2″-4′, 2′-3′
	sugar-base	–	1′-8, 2′-8	3′-8, 5′-8
3	intra-sugar	1′-2′, 2′-2″	2′-3′, 3′-5′	1′-4′, 2″-3′, 3′-4′
	sugar-base	–	2′-8	1′-8, 3′-8
	intra-side chain	*ortho-meta*	–	–
	sugar-side chain	–	–	1′-*ortho*

[a]2″, alpha (or down) proton; [b]2′, beta (or up) proton; [c]-, none observed.

Marcel Dekker, Inc.
270 Madison Avenue, New York, New York 10016

conformation since in the ap, $C_{3'}$ exo/endo conformation a weak but discernable NOE is expected. The medium sugar-base proton $H_{1'}$-H8 NOE argues against the *syn* conformation as an important contributor since this NOE is typically strong in the *syn* conformation. These results are consistent with the conformational analysis by potential energy calculation which gave high *anti* and +sc as the minimum energy conformations for torsional angle χ and γ, respectively, of **1**.

The sugar-base NOEs for **2** are very similar to that observed with **1** with one important exception. In this TCRTI the weak but discernable sugar-base proton $H_{5'}$-H8 NOE is most consistent with the ap conformation as indicated above. The medium sugar-base proton $H_{1'}$-H8 and $H_{2'}$-H8 NOEs, and the weak sugar-base proton $H_{3'}$-H8 NOE, are all consistent with a high anti conformer as with **1**. Thus this NMR data is also consistent with the calculated conformational preferences observed for **2**.

Most significantly, NOEs were observed between the protons of the sugar ring and the aromatic protons of the side chain phenyl ring for **1** (the phenyl ring of **2** lacks protons so this analysis is not possible). A medium NOE between $H_{1'}$ and the *ortho*-phenyl protons and a weak NOE between the *meta*-phenyl protons and $H_{4'}$ were observed, suggesting that **1** adopts an average conformation in which the side chain is folded toward the sugar ring. Consistent with this observation is the chemical shift of $H_{1'}$ in **1** which is shifted upfield by about 0.7 ppm to 5.7 ppm compared to other adenosine or $1,N^6$-etheno-adenosine analogues (δ $H_{1'} = 6.4$–6.5 ppm), suggesting that $H_{1'}$ in **1** is shielded by the aromatic ring. Of course other telling NOEs would have been between the side chain methylene with the $H_{1'}$ for the 180° Ψ_1 torsional angle or between the methylene and etheno α-H which would be indicative of a $+90/-90$ Ψ_1 conformer. Unfortunately, the chemical shift of the methylene proton resides under residual water, and thus this data can not be obtained.

3. Model Building and Docking

In order to examine the potential interactions between the enzyme and the nucleotide inhibitor, molecular modeling was performed by docking an energy minimum conformer of TCRTI **1** into the active site of HIV-1 RT. Construction of a three-dimensional model of TCRTI **1** was based on our results from conformational studies, which included a $C_{3'}$-exo sugar conformation, high anti glycosidic rotation, +sc conformation for γ, and fully extended conformations in the side chain with the exception of a Ψ_2 conformation of $-65°$ which was most consistent with the observed NOEs. Additionally, the conformation of the triphosphate group in the model was taken from the crystal structure of adenosine triphosphate[20] (the crystal structure of the ternary complex of HIV1 RT[21] was not available when this model was first created[22]).

The constructed model of TCRTI **1** was then docked into the active site of HIV-1 RT in MIDAS.[10] The structure of RT was taken from the 3.0 Å crystal structure of HIV-1 RT complexed with a 19-mer/18-mer template/primer and an antibody.[23] Since labeling studies show an active site specific labeling of HIV-1 RT by TCRTI **1** and covalent modification at Ser^{156},[5] the TCRTI was positioned in the DNA

Marcel Dekker, Inc.
270 Madison Avenue, New York, New York 10016

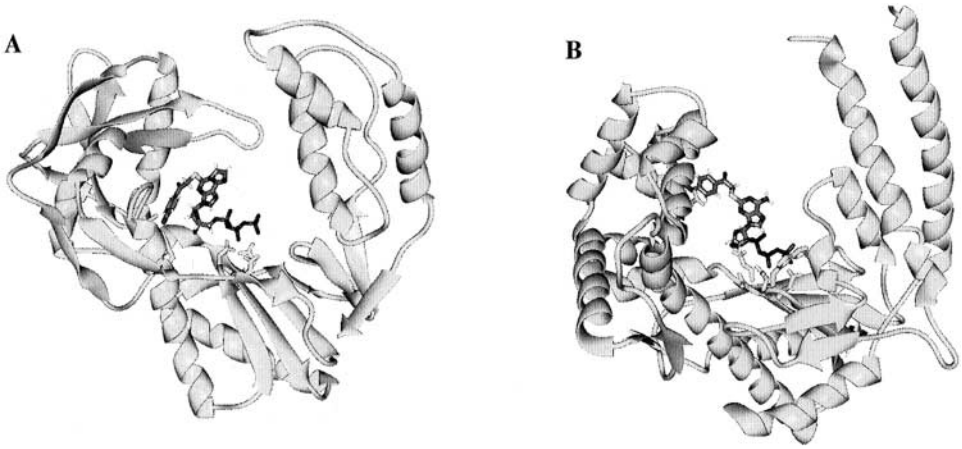

Figure 6. Models of **1** bound to RT (left) and **3** bound to Pol I (right). **A**. The RT complex is shown looking into the DNA cleft with the fingers subdomain on the left; **B**. The Pol I model is shown looking into the DNA binding cleft with the fingers domain to the left.

binding cleft with the side chain phenyl ring within bonding distance to this residue. Using this as an anchor point, the inhibitor was then rotated into the proposed active site in the palm subdomain. In doing so, the magnesium-complexed triphosphate of the inhibitor is in a proper orientation and distance to interact with the triphosphate binding site, that is, the β- and γ-phosphates interact with Asp^{110} and Asp^{185}, and the anhydride oxygen of the α-phosphate interacts with Asp^{186}, via magnesium chelation.[24] The resulting model of TCRTI **1** bound to the active site of RT, and for comparison the model of **3** bound to Pol I,[6] are given in Fig. 6.

The major interaction between the inhibitor and the enzyme in the model is from the triphosphate, sugar and the 2-position side chain. The base is positioned at the center of the cleft at a considerable distance from the fingers subdomain, but the 2-position side chain makes extensive contacts with amino acid residues Pro^{150}, Gin^{151}, Ser^{156}, Pro^{157}, and Phe^{160} in the template grip. In particular, the phenyl ring of Phe^{160}, which is located on the same face of α-helix E as Ser^{156}, is in close contact with the azidophenyl ring of TCRTI **1**, suggesting that it may be involved in inhibitor binding by hydrophobic interactions with the side chain phenyl ring. In addition, the backbone nitrogen of Gin^{151} is within hydrogen bonding distance with the side chain carbonyl group of the inhibitor. In addition to the three catalytically important carboxylates Asp^{110}, Asp^{185}, and Asp^{186}, residues Met^{184} and Asp^{113} are also in close proximity to the triphosphate moiety of the inhibitor and may play a role in binding. The sugar of the TCRTI is positioned in the cleft with the 3′-hydroxyl group pointing away from the exonuclease domain with the side chain of amino acid residues Ala^{114} and Tyr^{115} making Van der Waals contact with the sugar ring. In this regard it should be noted that this model, which was constructed before a crystal structure was available, provides a good overlay with the position of the TTP substrate observed in a subsequent covalent ternary complex.[21]

Marcel Dekker, Inc.
270 Madison Avenue, New York, New York 10016

CONCLUSIONS

Molecular mechanics calculations and 2-dimensional NMR spectroscopic studies indicate that the 2-position side chains of TCRTIs **1** and **2** and the polymerase inhibitor **3** exhibit significantly different conformational preferences. In TCRTIs **1** and **2**, the etheno group, particularly the N1-Cα and Cα-H bonds of the etheno group, force a 180 degree Ψ_1 rotation which projects the aromatic ring of the side chain down toward the sugar. On the other hand, the side chain of TCPI **3** favors an orientation with the aromatic ring extending out from the purine ring. Other conformational preferences observed for inhibitors **1**, **2** and **3** were similar, with sugar puckering preferences at $C_{2'}$-endo/$C_{3'}$-exo (south), the orientation of the base (χ) at high *anti*, and the orientation of the 5′-phosphate (γ) at +sc or ap. The absence of significant differences in the sugar and base conformations in these two classes of nucleotide inhibitors suggests that the differences in side chain conformations predicted in the molecular mechanics calculations and observed in the NMR studies result in different binding interactions at the active sites of HIV-1 RT and Pol I.

The preferred side chain conformations for the TCRTI vs. TCPI inhibitors can also be seen in the models of bound inhibitor. In the model of reverse transcriptase bound to **1**, the side chain makes contact with the template grip region at the juncture of the palm and finger domains of the polymerase active site. The model of Pol I bound to **3** (also shown in Fig. 6) shows that the side chain must extend out from the purine ring to make contact with the fingers domain well above the palm/finger interface. Thus the selectivities of these inhibitors are also related to the absence or presence of lipophilic binding sites for the preferred side chain conformations. The presence of these specific side chain binding sites provides reasonable expectations that very specific inhibitors can be developed for different types and classes of these polymerases.

REFERENCES

1. Van Roey, P.; Taylor, E.W.; Chu, C.K.; Schinazi, R.F. Conformational analysis of 2′,3′-didehydro-2′,3′-dideoxypyrimidine nucleosides. J. Am. Chem. Soc. **1993**, *115*, 5365–5371.
2. Jagannadh, B.; Reddy, D.V.; Kunwar, A.C. 1H NMR study of the sugar pucker of 2′,3′-dideoxynucleosides with anti-human immunodeficiency virus (HIV) activity. Biochem. Biophys. Res. Commun. **1991**, *179*, 386–391.
3. Li, K.; Lin, W.; Chong, K.H.; Moore, B.M.; Doughty, M.B. Template-competitive inhibitors of HIV-1 reverse transcriptase: Design, synthesis and inhibitory activity. Bioorganic and Medicinal Chemistry **2002**, *10*, 507–515.
4. Moore, B.M.; Li, K.; Doughty, M.B. Deoxyadenosine-based DNA polymerase photoprobes: Design, synthesis and characterization as inhibitors of DNA polymerase I Klenow fragment. Biochemistry **1996**, *35*, 11,634–11,641.

Marcel Dekker, Inc.
270 Madison Avenue, New York, New York 10016

5. Lin, W.; Li, K.; Doughty, M. Characterization of a binding site for template competitive inhibitors of HIV-1 reverse transcriptase using photolabeling derivatives. Bioorganic and Medicinal Chemistry **2002**, *10*, 4131–4141.
6. Moore, B.M.; Jalluri, R.; Doughty, M.B. DNA Polymerase photoprobe 2-(4-azidophenacyl)thio-dATP identifies the template binding region of the DNA polymerase I Klenow fragment. Biochemistry **1996**, *36*, 11,642–11,651.
7. Weiner, S.J.; Kollman, P.A.; Case, D.A.; Singh, U.C.; Ghio, C.; Alagona, G.; Profeta, S.; Weiner, P. A new force field for molecular mechanical simulation of nucleic acids and proteins. J. Am. Chem. Soc. **1984**, *106*, 765–784.
8. Weiner, S.J.; Kollman, P.A.; Nguyen, D.T.; Case, D.A. An all atom force field for simulations of proteins and nucleic acids. J. Computational Chem. **1985**, *7*, 230–252.
9. Jalluri, R.K.; Yuh, Y.H.; Taylor, E.W. O-C-N anomeric effect in nucleosides: A major factor underlying the experimentally observed eastern barrier to pseudorotation. In *The Anomeric Effect and Associated Steroelectronic Effects*; Thatcher, G.R.J., Ed.; American Chemical Society: Washington, 1993; 277–293.
10. Ferrin, T.E.; Huang, C.C.; Jarvis, L.E.; Langridge, R. The MIDAS display system. J. Mol. Graphics **1988**, *6*, 13–27.
11. Abola, E.E.; Bernstein, F.C.; Bryant, S.H.; Koetzle, T.F.; Weng, J. Protein data bank. In *Crystallographic Databases-Information Content, Software Systems, Scientific Applications*; Allen, F.H., Bergerhoff, G., Sievers, R., Eds.; Data Commission of the International Union of Crystallography: Bonn/Cambridge/Chester, 1987; 107–132.
12. Slessor, K.N.; Tracey, A.S. Couplings into methylene groups: A NOE nuclear magnetic resonance approach to stereochemistry. Can. J. Chem. **1970**, *49*, 2874–2884.
13. Haasnoot, C.A.G.; de Leeuw, F.A.A.M.; de Leeuw, H.P.M.; Altona, C. The relationship between proton-proton NMR coupling constants and substituent electronegativities. II. Conformational analysis of the sugar ring in nucleosides and nucleotides in solution using a generalized Karplus equation. Org. Magn. Reson. **1981**, *15*, 43–52.
14. de Leeuw, F.A.A.M.; Altona, C. Computer-assisted pseudorotational analysis of five membered rings by means of proton spin-spin coupling constants: Program PSEUROT. J. Comp. Chem. **1983**, *4*, 428–437.
15. Painter, P.G.; Aulabaugh, A.E.; Andrews, C.W. A comparison of the conformations of the 5′-triphosphate of zidovudine (AZT) and thymidine bound to HIV-1 reverse transcriptase. Biochem. Biophy. Res. Commun. **1993**, *191*, 1166–1171.
16. Saenger, W. Structure and function of nucleosides and nucleotides. Agnew. Chem. Int. Ed. Engl. **1973**, *12*, 591–601.
17. Arnott, S.; Hukins, D.W.L. Refinement of the structure of B-DNA and implications for the analysis of X-ray diffraction data of biopolymers. J. Mol. Biol. **1973**, *81*, 93–105.

Marcel Dekker, Inc.
270 Madison Avenue, New York, New York 10016

18. de Leeuw, H.P.M.; Haasnoot, C.A.G.; Altona, C. Empirical correlations between conformational parameters in β-D-furanoside fragments derived from a statistical survey of crystal structures of nucleic acid constituents. Full description of nucleoside molecular geometries in terms of four parameters. Isr. J. Chem. **1980**, *20*, 108–126.
19. Wuthrich, K. Nuclear overhauser enhancement (NOE) in biopolymers. In *NMR of Proteins and Nucleic Acid*; John Wiley & Sons: New York, 1986; 93–113.
20. Kennard, O.; Isacs, N.W.; Motherwell, W.D.S.; Coppola, J.C.; Wampler, D.L.; Larson, A.C.; Watson, D.G. The crystal and molecular structure of adenosine triphosphate. Proc. R. Soc. Lond. A. **1971**, *325*, 401–436.
21. Huang, H.; Chopra, R.; Verdine, G.L.; Harrison, S.C. Structure of a covalently trapped catalytic complex of HIV-1 reverse transcriptase: Implications for drug resistance. Science **1998**, *282*, 1669–1675.
22. Li, K. *Identification of HIV-1 Reverse Transcriptase Substrate Binding Sites by a Selective Nucleotide Photoprobes: Implications for Inhibitor Design*, Ph.D., Department of Medicinal Chemistry, University of Kansas, **1996**, 226.
23. Jacobo-Molina, A.; Ding, J.; Nanni, R.G.; Clark, A.D.; Lu, X.; Tantillo, C.; Williams, R.L.; Kamer, G.; Ferris, A.L.; Clark, P.; Hizi, A.; Hughes, S.H.; Arnold, E. Crystal structure of human immunodeficiency virus type 1 reverse transcriptase complexed with double-stranded DNA at 3.0 Å resolution shows bent DNA. Proc. Natl. Acad. Sci. USA **1993**, *90*, 6320–6324.
24. Patel, P.H.; Jacobo-Molina, A.; Ding, J.; Tantillo, C.; Clark, A.D.; Raag, R.; Nanni, R.G.; Hughes, S.H.; Arnold, E. Insights into DNA polymerization mechanisms from structure and function analysis of HIV-1 reverse transcriptase. Biochemistry **1995**, *34*, 5351–5363.

Received September 19, 2002
Accepted January 27, 2003

MARCEL DEKKER, INC.
270 Madison Avenue, New York, New York 10016

MARCEL DEKKER, INC.
270 Madison Avenue, New York, New York 10016